



## Secular period increase and improved quadratic ephemeris of the eclipsing binary MoV62 Cyg = CzeV1391

Reffke, Udo – Bad Zwischenahn, Germany  
email: [UR.Reffke@web.de](mailto:UR.Reffke@web.de)

Bernhard, Klaus - Linz, Austria  
email: [Klaus1967Bernhard@gmx.at](mailto:Klaus1967Bernhard@gmx.at)

Moschner, Wolfgang - Lennestadt, Germany  
email: [wolfgang.moschner@gmx.de](mailto:wolfgang.moschner@gmx.de)

Frank, Peter - Velden, Germany  
email: [frank.velden@t-online.de](mailto:frank.velden@t-online.de)

Bundesdeutsche Arbeitsgemeinschaft für Veränderliche Sterne e.V.

December 2025

**Abstract:** *The variability of MoV62 Cyg = CzeV1391 was independently discovered in 2017 by Wolfgang Moschner and Zbynek Henzl, who classified it as an eclipsing binary. We analyse available minima timings covering the interval from JD 2457574 to JD 2460934 (2016-2025), complemented by our CCD photometry and public survey data from VSX, ATLAS, ZTF, and Gaia. Linear ephemerides based on the published survey periods produce pronounced parabolic trends in the O-C diagrams, demonstrating that the orbital period is not constant. A single global quadratic ephemeris removes this curvature and yields nearly flat O-C residuals over the full time span. The authors present phased light curves from ZTF and their own data, a list of primary and secondary minima, O-C diagrams, and an improved global period solution of the star. Continued monitoring is recommended to further constrain the long-term evolution of the orbital period and to test for possible cyclic contributions.*

### Observations

400 mm ASA Astrograph f/3.7 - f = 1471 mm, FLI Proline 16803 CCD-Camera - V-filter - t = 120 sec.  
Wolfgang Moschner, Astrocamp/Nerpio, Spain

### Data analysis

MuniWin [1] and self-written programs by Franz Agerer and Lienhard Pagel [2] were used for the analysis of the frames, after bias, dark and flatfield correction. The weighted average of 5 comparison stars was used.

### Explanations:

HJD = heliocentric UTC timings (JD) of the observed minima

All coordinates are taken from the Gaia DR3 catalogue [3]. The coordinates (epoch J2000) are computed by VizieR, and are not part of the original data from Gaia (note that the coordinates are computed from the positions and the proper motions).

### MoV62 Cyg

Cross-IDs

= ZTF J201623.20+522909.9

= ATO J304.0966+52.4860

= Gaia DR3 2184376184429225472

= UCAC4 713-071405

= 2MASS J20162319+5229097

= UCAC3 285-157675

= CzeV1391

**Gaia DR3 catalogue:**

Right ascension: 20h16m23.1941s      at Epoch J2000  
 Declination: +52° 29' 09.788"      at Epoch J2000

15.2705 mag G-band mean magnitude (350-1000 nm)  
 15.6190 mag Integrated BP mean magnitude (330-680 nm)  
 14.7370 mag Integrated RP mean magnitude (640-1000 nm)  
 0.8820 mag BP-RP

**Periods known so far:**

VSX [4]	0.3526412 d	ATLAS [6]	0.352636 d
ASAS-SN	no information	WISE	no information
ZTF g-band [5]	0.3526436 d	Gaia [7]	0.3526414 d
ZTF r-band [5]	0.3526392 d		

**Results**

MoV62 Cyg = CzeV1391 was independently identified as a previously unreported variable star in 2017 during CCD observations of a nearby main target. Subsequent measurements confirmed its EW type light curve morphology, and the object was reported to the AAVSO VSX database. An independent discovery was later published as CzeV1391, demonstrating that the system had not previously been catalogued. The presence of well defined primary and secondary minima made the object suitable for a long-term timing analysis.

Figure 1 summarises the final global quadratic timing solution for comparison, O-C diagrams based on linear ephemerides from surveys and local CCD subsets are shown in Figures 2–7. The complete set of available minima timings, covering the interval from JD 2457574 to JD 2460934 (corresponding to the years 2016 → 2025), shows clear systematic deviations from all linear ephemerides based on archival survey periods derived from the VSX, ATLAS, ZTF, and Gaia databases (see Figures 2–7). Linear ephemerides were examined explicitly as an alternative description, motivated by the possibility of a discrete period change. Two additional local linear ephemerides were derived from our CCD minima subsets (2018–2021 and 2022–2025) by a least-squares fit. Secondary minima were treated under the standard EW assumption that Min. II occurs at phase 0.5. Figures 2 and 3 illustrate the two piecewise linear comparison solutions derived from the 2022–2025 and 2018–2021 subsets, while Figures 4–7 show O–C diagrams based on published survey periods (VSX, ATLAS, ZTF, Gaia). However, each linear solution produces a pronounced parabolic trend in the corresponding O–C diagram, demonstrating that a constant-period model cannot account for the observed timing behaviour. The periods obtained from the early and late CCD subsets (Figures 2 and 3) differ by about 0.36 s, which is of the same order as expected from the secular trend implied by the quadratic timing solution.

In order to accommodate this systematic curvature, the timings were described by means of a quadratic ephemeris of the general form

$$T(E) = T_0 + P_0 \cdot E + Q \cdot E^2.$$

A least-squares fit of this formalism to all available minima, including the timings listed in Table 1, the supplementary minima set provided in the working file, and additional minima extracted from ATLAS and ZTF data yields a single global solution that reproduces the observations over the entire time span. When this quadratic ephemeris is applied, the resulting O–C diagram (Figure 1) becomes flat and shows only small, symmetric residuals around zero, indicating that the long term timing behaviour of MoV62 Cyg is well represented by a continuous period evolution rather than by a sudden period jump.

The quadratic term of the ephemeris implies a steadily increasing orbital period. The analysis shows that the orbital period of the system is increasing at a very small but measurable rate, fully comparable to the secular period changes typically observed in EW type contact binaries. From the quadratic ephemeris fit, we infer a small but measurable secular increase of the orbital period of approximately 0.07 s per year over the observed interval; this value should be regarded as a formal, unweighted estimate given the lack of homogeneous timing uncertainties for the individual minima. This value represents a mean rate over the observed interval; the instantaneous period change per individual cycle is much smaller and becomes measurable only through accumulation over the multi year baseline.

To avoid perplexity, we emphasise that this value is a mean rate per year; the change per individual orbital cycle is much smaller and becomes measurable only through accumulation over the multi year time baseline.

This rate corresponds to a gradual lengthening of the orbital cycle over time, consistent with evolutionary processes such as mass transfer or angular momentum redistribution within the system.

This gradual period increase can plausibly be attributed to ongoing mass transfer and/or angular momentum redistribution driven by magnetic activity within the system. While a detailed physical modelling of these processes is beyond the scope of the present study, the observed trend clearly reflects an evolutionary timescale characteristic of interacting close binaries.

The complete list of primary and secondary minima calculated with the quadratic elements is presented in Table 1. The residuals are confined to a narrow range and show no remaining systematic trends, which confirms the adequacy of the quadratic description. The O–C values of the secondary minima were computed under the approximation of a phase offset of exactly 0.5. No systematic deviations between primary and secondary minima are detected, indicating that this assumption is valid for the present EW type system.

The phased light curve obtained from our own CCD observations in 2017 (Figure 8) confirms the EW type morphology of MoV62 Cyg. Independent ZTF r-band data (Figures 9 and 10) reproduce the same light curve structure and significantly extend the temporal coverage of the system. Long-term variations of low amplitude visible in the ZTF photometry appear to be correlated with the secular period increase. At present, however, this correlation remains purely empirical, and its physical origin requires further investigation.

While the quadratic ephemeris fully accounts for the currently observed O–C behaviour, a possible light time effect caused by a distant third body cannot yet be excluded. A substantially longer observational baseline will be required to distinguish conclusively between a purely secular trend and a possible long-period cyclic modulation. Continued photometric monitoring of MoV62 Cyg is therefore strongly recommended.

### Summary on uncertainties

Formal uncertainty estimates for individual minima cannot be given on a uniform statistical basis, as the relevant public databases (VSX, ATLAS, ZTF, and Gaia) do not provide consistently defined timing errors. Therefore, individual minima could not be assigned homogeneous timing uncertainties for a uniform weighted solution; the quoted ephemeris uncertainties are formal fit errors derived from the adopted least-squares procedure. The evidence for a continuous secular period evolution therefore rests on the global parabolic structure of the linear O–C diagrams and on its complete suppression by the quadratic ephemeris.

**MoV62**            **calculated with Quadratic Ephemeris (Bernhard 2025)**  
Type    =    EW  
Min. I   =    HJD 2459788.5734 + 0.352642454\*E+3.70(33)\*10<sup>−10</sup>\*E<sup>2</sup>.  
                 ±0.0004   ±0.000000013

Observer	HJD-Date Minimum	Type	Epoch	O-C (d)	Source
W. Moschner	2457574.5230	II	-6278.5	0.0001	
W. Moschner	2457576.4623	I	-6273	-0.0001	
W. Moschner	2457581.5713	II	-6258.5	-0.0043	
W. Moschner	2457605.3787	I	-6191	0.0000	
W. Moschner	2457605.5518	II	-6190.5	-0.0032	
W. Moschner	2457623.3637	I	-6140	0.0005	
W. Moschner	2457623.5402	II	-6139.5	0.0006	
W. Moschner	2457691.4224	I	-5947	0.0000	
W. Moschner	2457916.5846	II	-5308.5	0.0027	
W. Moschner	2457955.5481	I	-5198	-0.0004	
W. Moschner	2457963.4863	II	-5175.5	0.0035	
W. Moschner	2457963.6553	I	-5175	-0.0039	
W. Moschner	2457979.5252	I	-5130	-0.0027	
W. Moschner	2458010.3880	II	-5042.5	0.0042	
W. Moschner	2458010.5625	I	-5042	0.0024	
W. Moschner	2458015.3194	II	-5028.5	-0.0013	
W. Moschner	2458015.5006	I	-5028	0.0036	

W. Moschner	2458329.5236	II	-4137.5	0.0015	
W. Moschner	2458330.4056	I	-4135	0.0019	
W. Moschner	2458330.5813	II	-4134.5	0.0013	
W. Moschner	2458352.4455	II	-4072.5	0.0018	
Zbyněk Henzl	2458381.3585	II	-3990.5	-0.0016	CzeV catalog
Zbyněk Henzl	2458382.4138	II	-3987.5	-0.0042	CzeV catalog
W. Moschner	2458397.4043	I	-3945	-0.0009	
W. Moschner	2458720.4227	I	-3029	-0.0007	
W. Moschner	2458720.6017	II	-3028.5	0.0020	
W. Moschner	2458755.3362	I	-2930	0.0015	
W. Moschner	2458755.5126	II	-2929.5	0.0015	
W. Moschner	2459053.4930	II	-2084.5	0.0006	
W. Moschner	2459053.6650	I	-2084	-0.0037	
W. Moschner	2459069.3647	II	-2039.5	0.0035	
W. Moschner	2459069.5360	I	-2039	-0.0015	
W. Moschner	2459102.5078	II	-1945.5	-0.0017	
W. Moschner	2459140.4191	I	-1838	0.0007	
W. Moschner	2459403.4887	I	-1092	-0.0001	
W. Moschner	2459426.4095	I	-1027	-0.0010	
W. Moschner	2459426.5849	II	-1026.5	-0.0020	
W. Moschner	2459469.4310	I	-905	-0.0018	
W. Moschner	2459777.4628	II	-31.5	-0.0029	
W. Moschner	2459777.6411	I	-31	-0.0009	
W. Moschner	2459788.3993	II	-0.5	0.0017	
W. Moschner	2459788.5734	I	0	-0.0005	
W. Moschner	2459853.4616	I	184	0.0014	
W. Moschner	2460143.5089	II	1006.5	-0.0001	
W. Moschner	2460159.3759	II	1051.5	-0.0020	
W. Moschner	2460159.5560	I	1052	0.0018	
W. Moschner	2460178.4196	II	1105.5	-0.0010	
W. Moschner	2460178.5988	I	1106	0.0018	
W. Moschner	2460213.3306	II	1204.5	-0.0017	
W. Moschner	2460213.5100	I	1205	0.0014	
W. Moschner	2460516.4287	I	2064	-0.0009	
W. Moschner	2460516.6066	II	2064.5	0.0007	
W. Moschner	2460525.4236	II	2089.5	0.0016	
W. Moschner	2460525.5984	I	2090	0.0001	
W. Moschner	2460566.3281	II	2205.5	-0.0006	
W. Moschner	2460566.5065	I	2206	0.0015	
W. Moschner	2460855.4960	II	3025.5	-0.0011	
W. Moschner	2460869.4266	I	3065	0.0001	
W. Moschner	2460869.6053	II	3065.5	0.0024	
W. Moschner	2460879.4744	II	3093.5	-0.0025	
W. Moschner	2460893.5838	II	3133.5	0.0011	
W. Moschner	2460918.4442	I	3204	0.0000	
W. Moschner	2460934.4893	II	3249.5	-0.0002	

Table 1: Minima of MoV62 Cyg = CzeV1391 calculated with Quadratic Ephemeris.  
The O-C of the secondary minima were calculated assuming that the true phase is at exactly at 0.5.

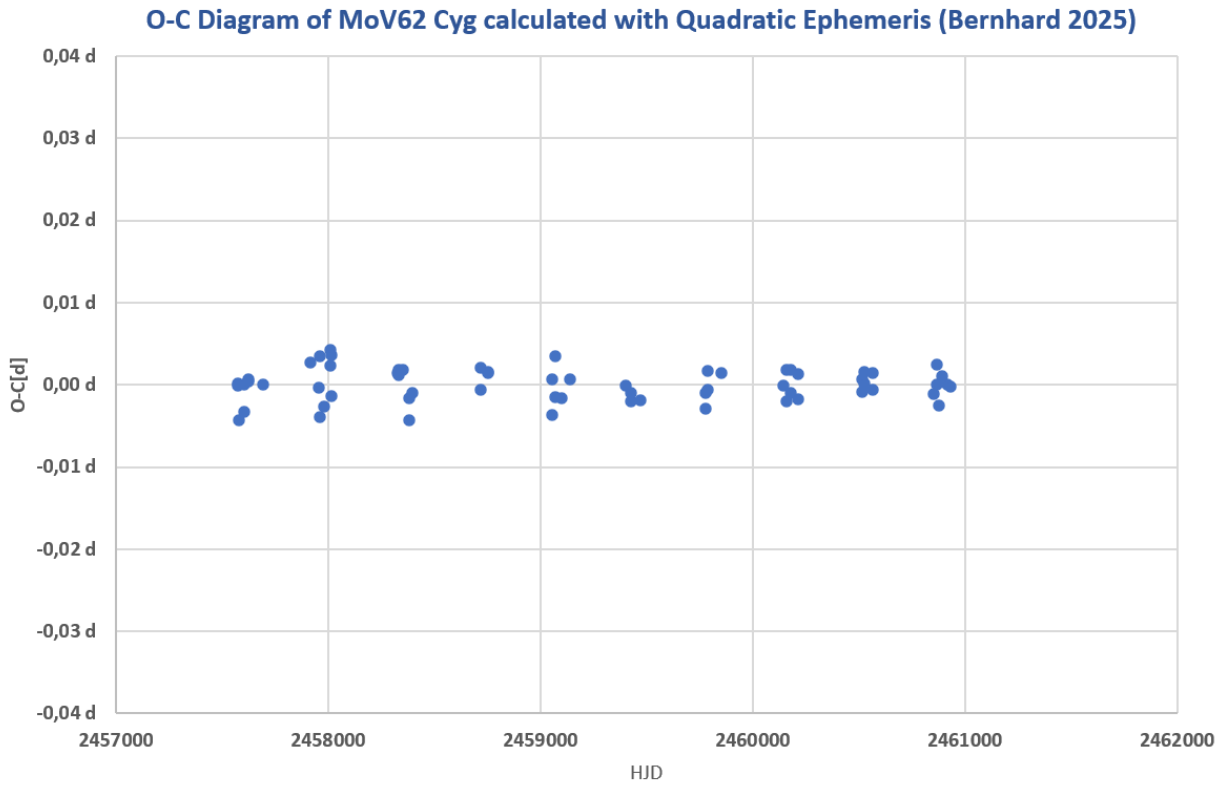


Figure 1: O-C-diagram of MoV62 Cyg = CzeV1391 calculated with Quadratic Ephemeris (Bernhard 2025).

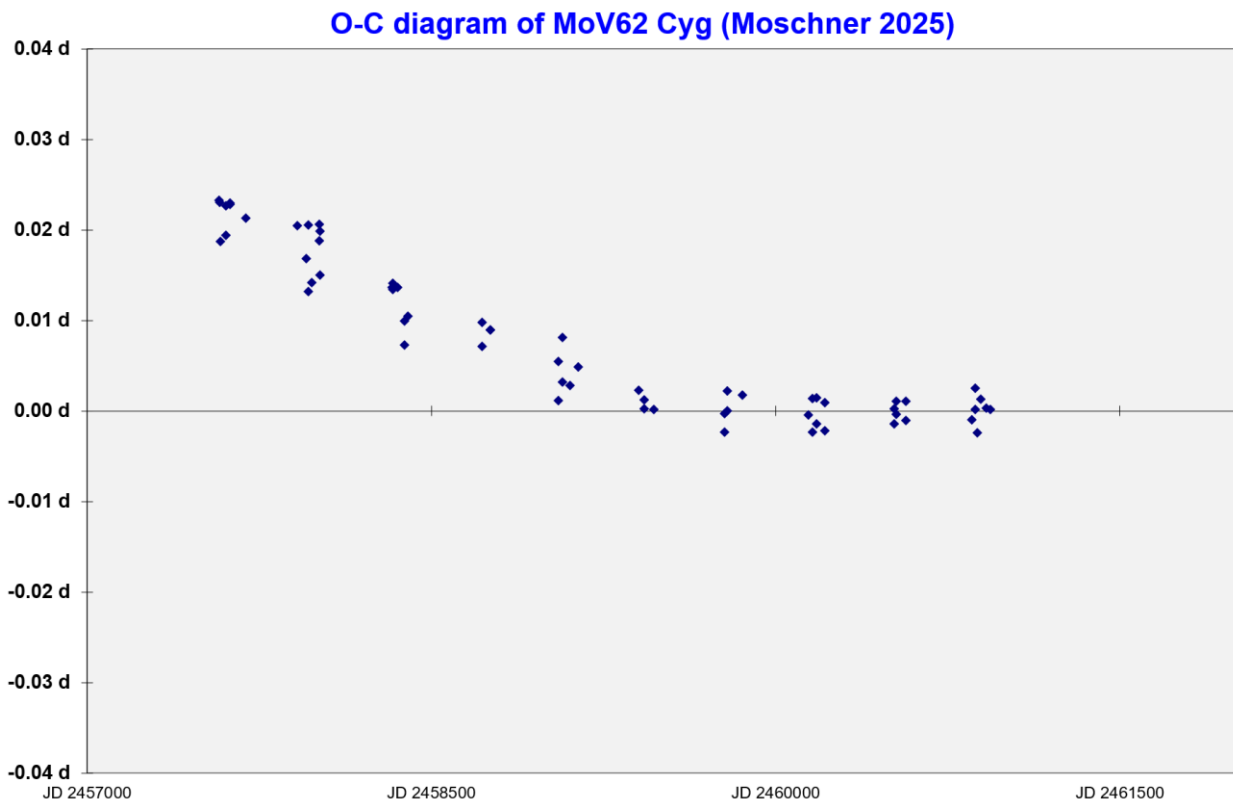


Figure 2: O-C diagram of MoV62 Cyg = CzeV1391 using a linear ephemeris fitted to the late CCD minima subset (2022-2025). These piecewise linear elements (period = 0.35264373 d) are shown for comparison and provide local fits only. The full data set is better represented by the global quadratic ephemeris (Figure 1).

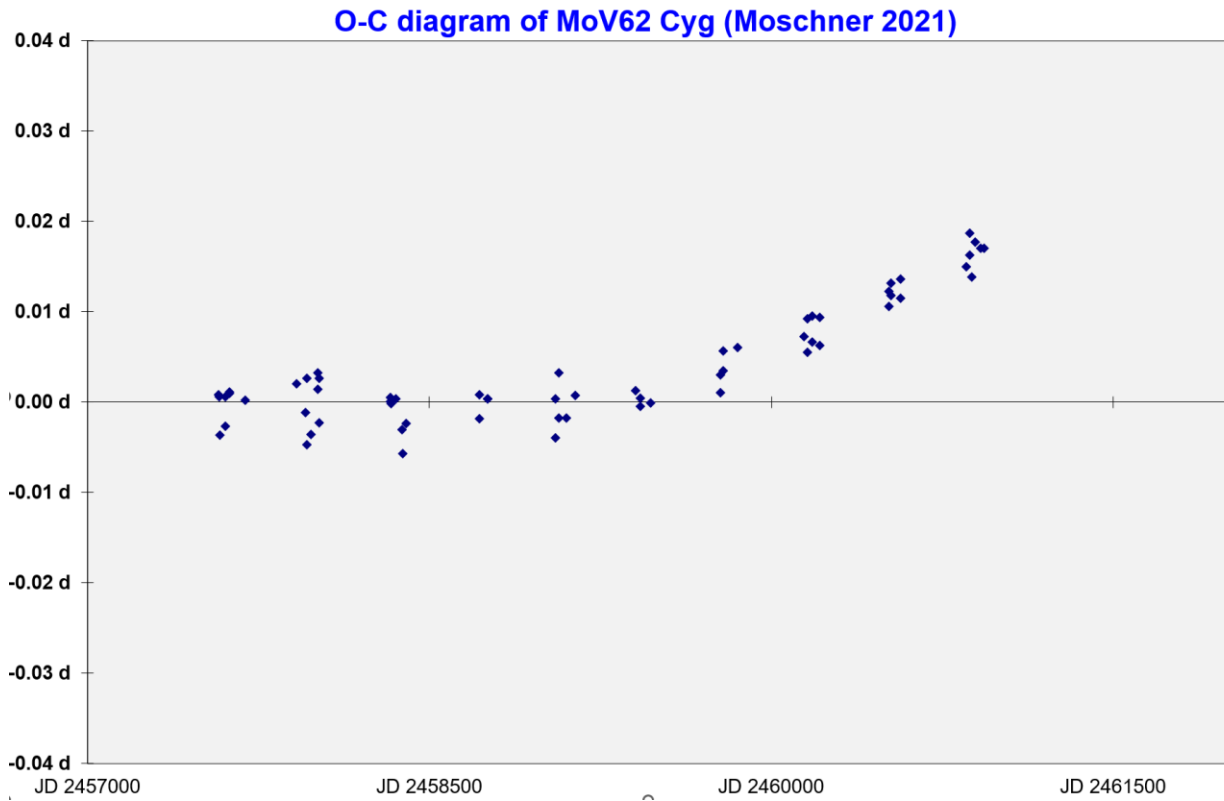


Figure 3: O-C diagram of MoV62 Cyg = CzeV1391 using a linear ephemeris fitted to the early CCD minima subset (2018-2021). These piecewise linear elements (period = 0.3526396 d) are shown for comparison and provide local fits only. The full data set is better represented by the global quadratic ephemeris (Figure 1).

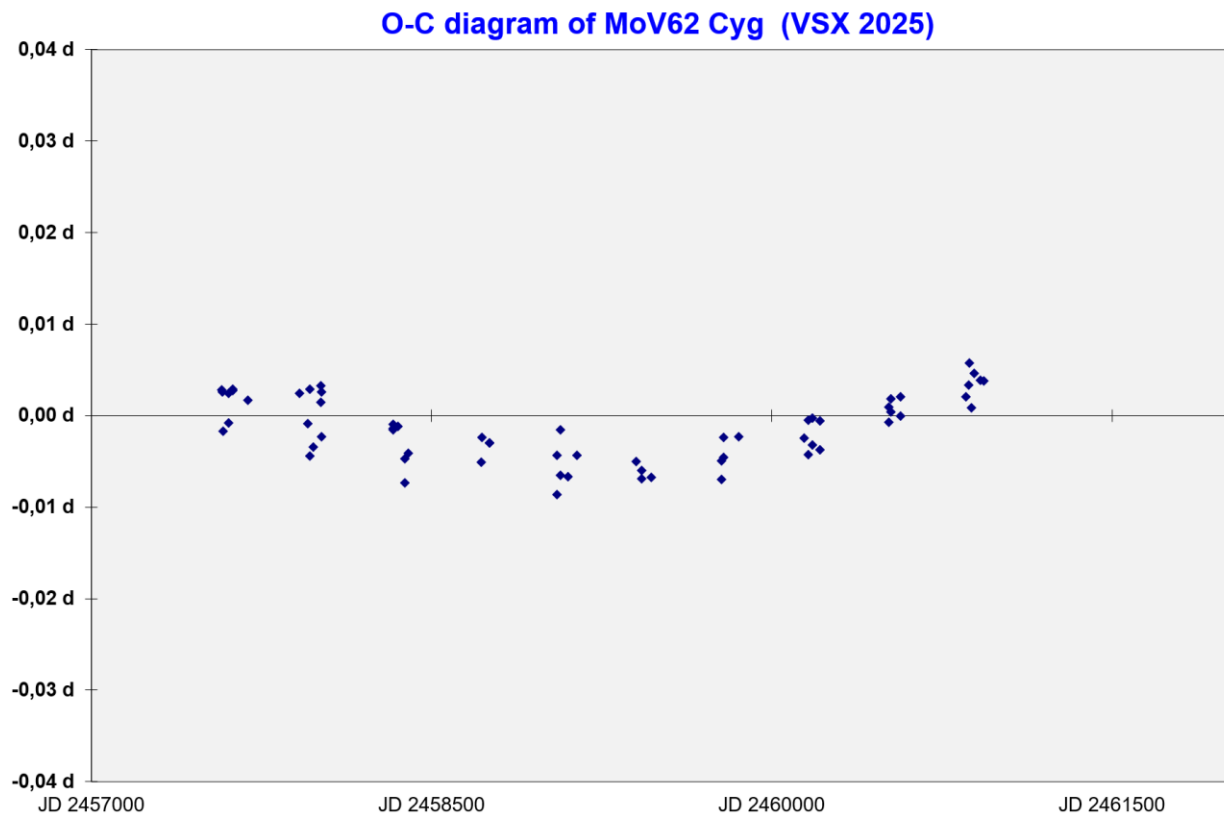


Figure 4: O-C-diagram of MoV62 Cyg = CzeV1391 using the period with linear elements from the VSX database and the Czech Variable Star Catalogue, 2018.

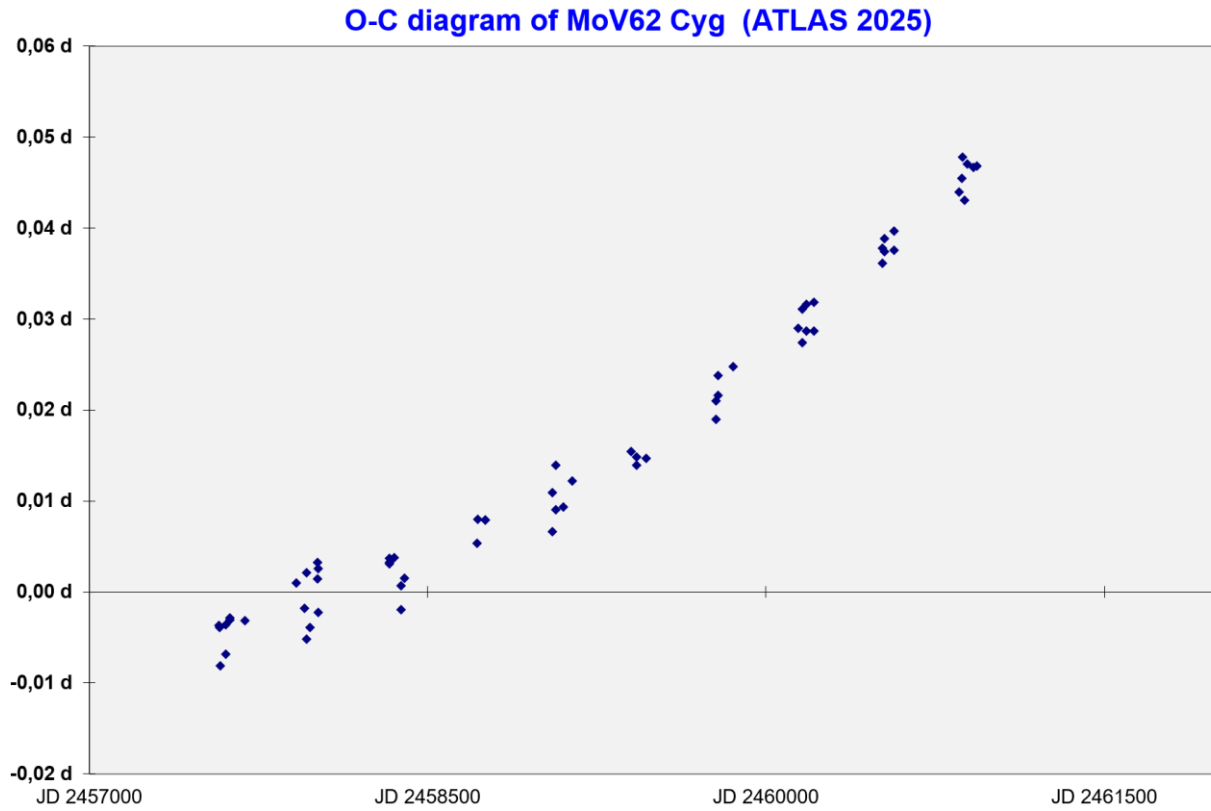


Figure 5: O-C-diagram of MoV62 Cyg = CzeV1391 using the period with linear elements from the ATLAS database.

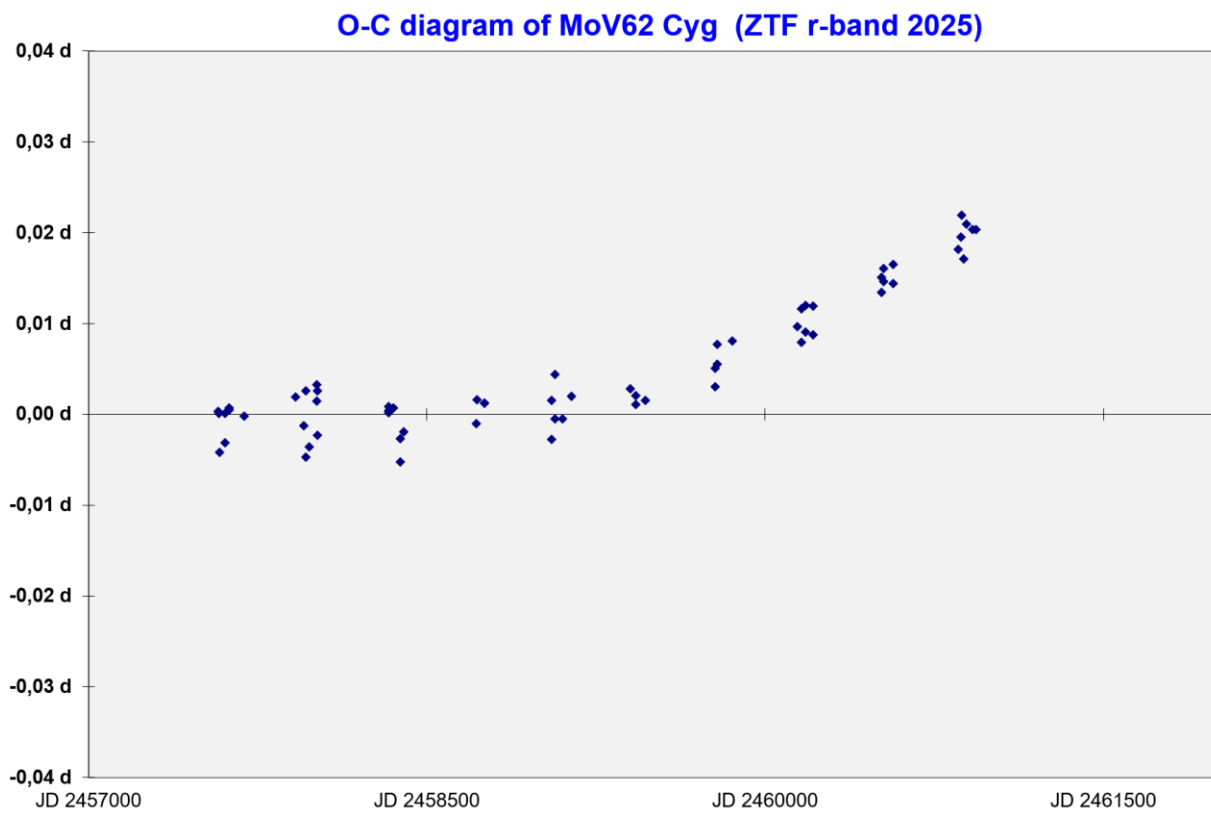


Figure 6: O-C-diagram of MoV62 Cyg = CzeV1391 using the period with linear elements from the ZTF database (r-band).

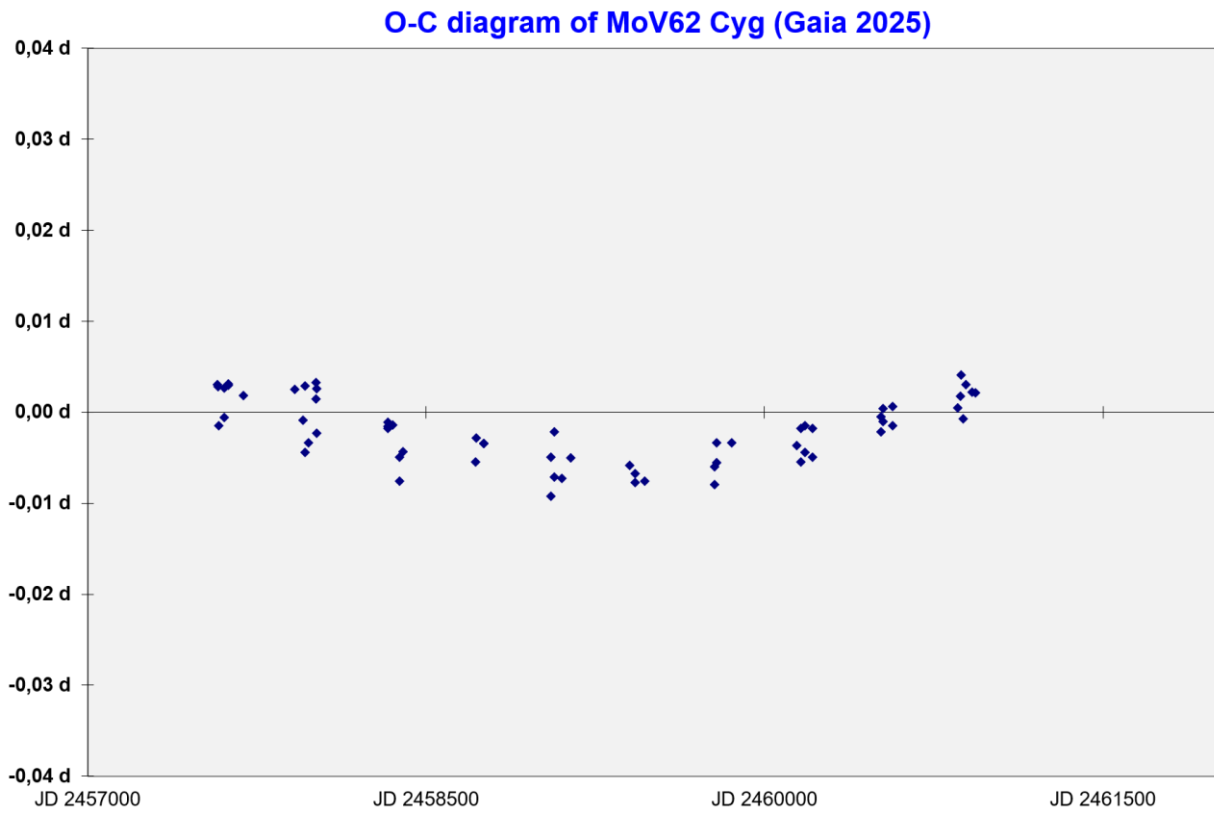


Figure 7: O-C-diagram of MoV62 Cyg = CzeV1391 using the period with linear elements from the Gaia database.

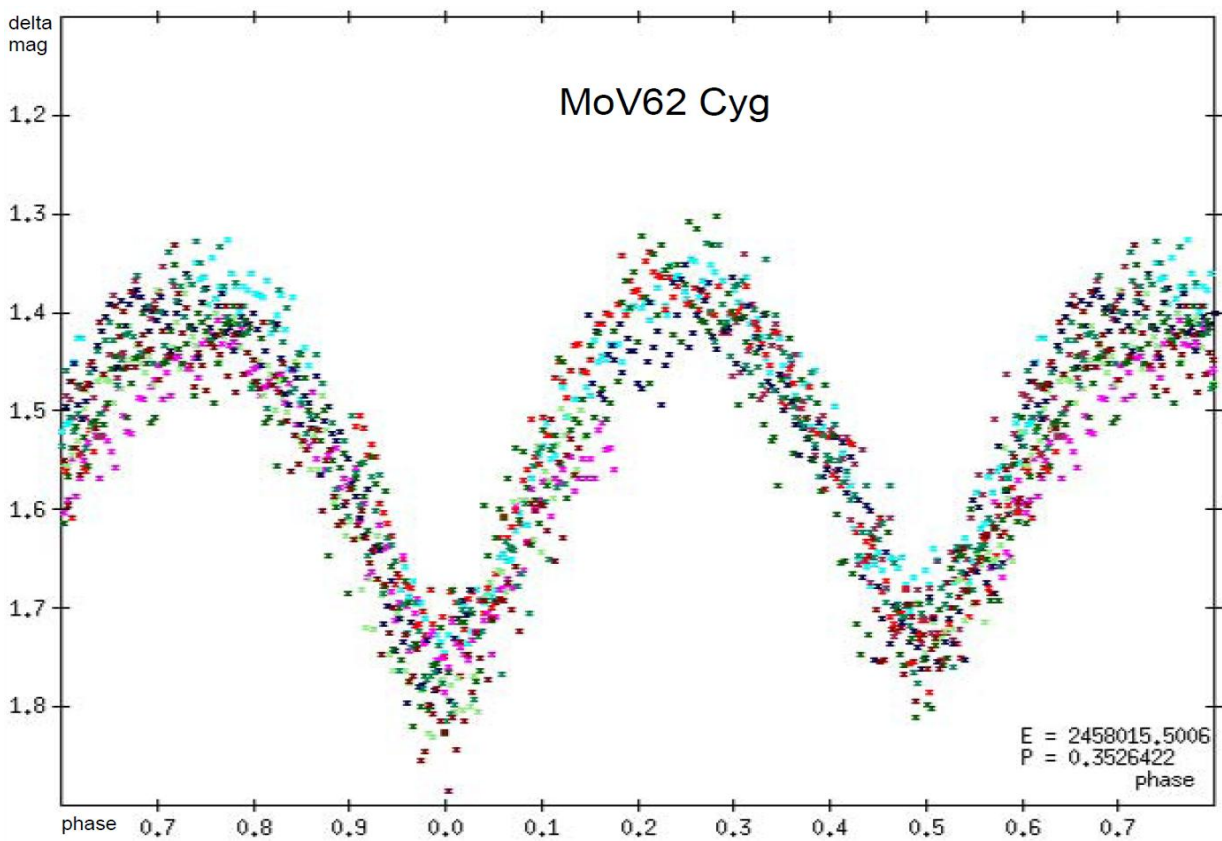


Figure 8: Phased lightcurve of MoV62 Cyg = CzeV1391 with the data (year 2017) from our telescope in Nerpio/Spain (V-Filter) and the first preliminary period.



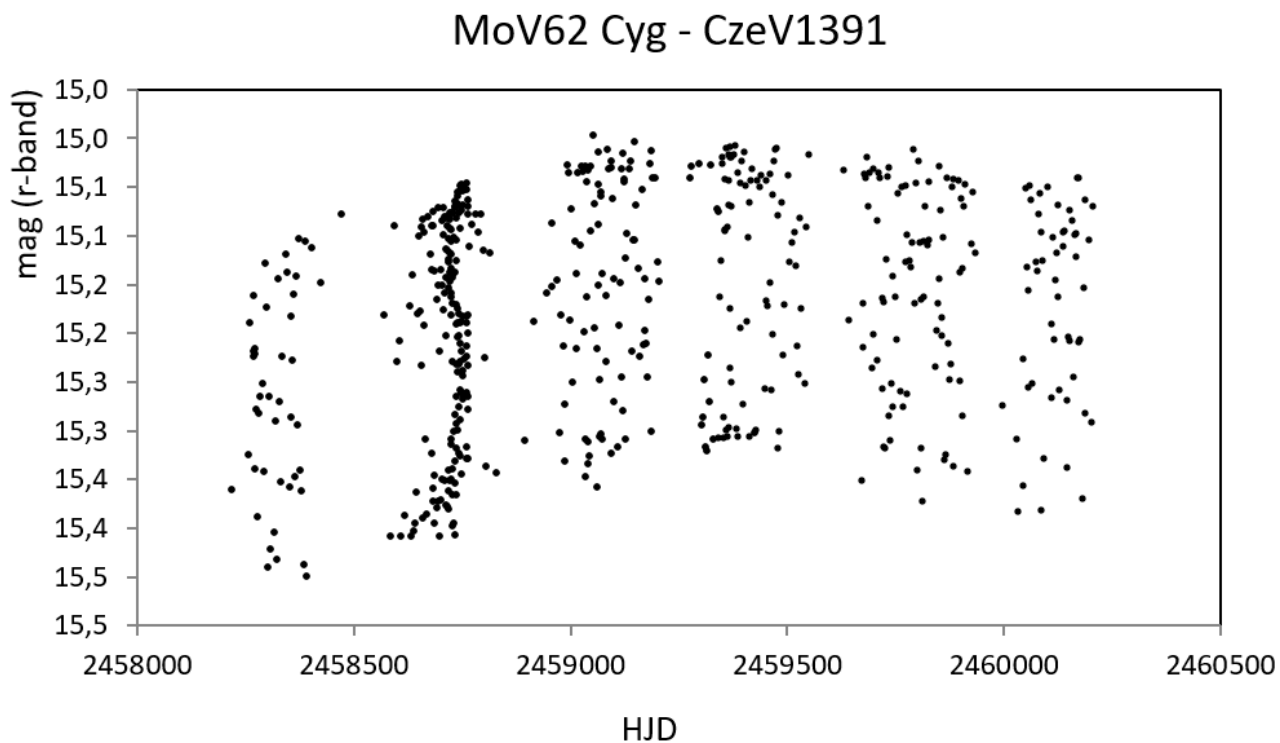


Figure 9: MoV62 Cyg = CzeV1391 data from the ZTF project (r-band)

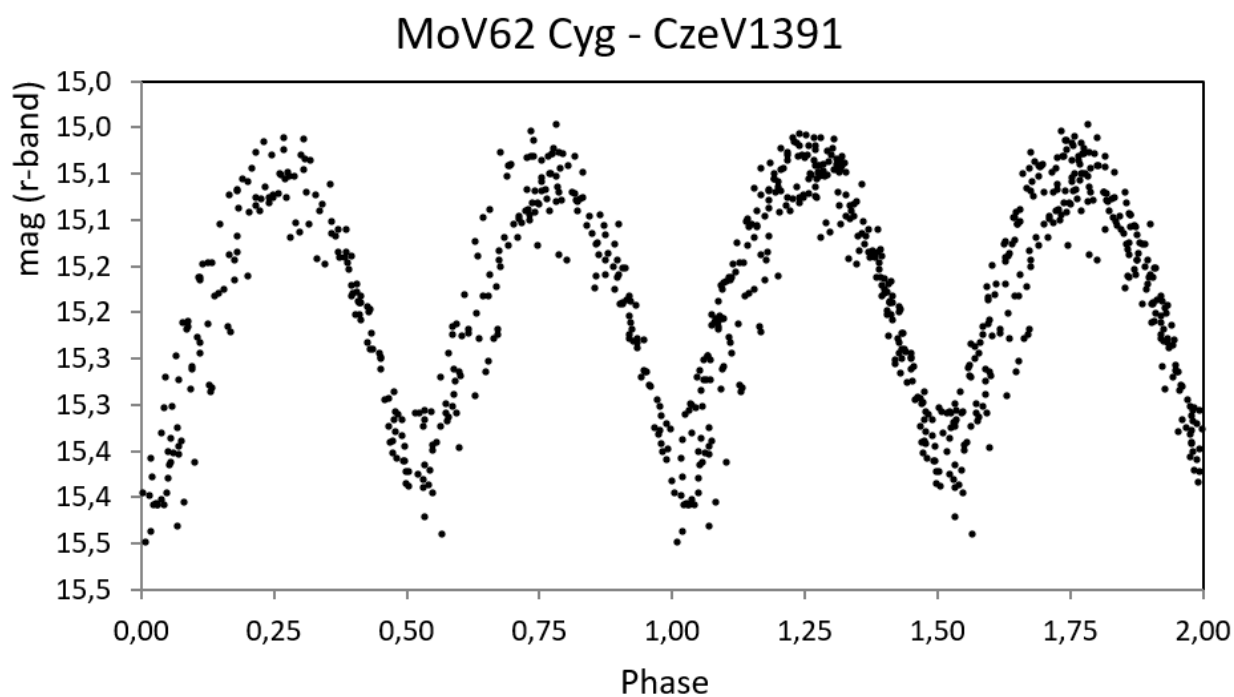


Figure 10: Phased lightcurve of MoV62 Cyg = CzeV1391 with the data and ephemeris with linear elements from the ZTF project (r-band).

## Acknowledgements

This research has made use of the SIMBAD database, operated at CDS, Strasbourg, France, the International Variable Star Index (VSX) database, operated at AAVSO, Cambridge, Massachusetts, USA, the Gaia Project, operated by European Space Agency, the ATLAS-Project developed by the University of Hawaii and funded by NASA, the ZTF-Project, operations are conducted by COO, IPAC and University of Washington.

The authors thank David Motl for providing his MuniWin photometry program, Franz Agerer (BAV) and Lienhard Pagel (BAV) for providing their personal data analysis program.

## References

- [1] Motl, David: MuniWin  
<http://c-munipack.sourceforge.net>
- [2] Pagel, Lienhard: Starcurve  
<https://www.bav-astro.eu/index.php/weiterbildung/tutorials>
- [3] Gaia DR3 (Gaia Collaboration. 2020) European Space Agency.  
<http://vizier.u-strasbg.fr/viz-bin/VizieR?-source=I/355>
- [4] The International Variable Star Index (VSX)  
<https://vsx.aavso.org/index.php?view=detail.top&oid=1544236>
- [5] ZTF Zwicky Transient Facility, Systematic Exploration of the Dynamic Sky  
<https://www.ztf.caltech.edu/>
- [6] A first catalog of variable stars measured by ATLAS (Heinze+, 2018)  
<http://vizier.u-strasbg.fr/cgi-bin/VizieR-3?-source=J/AJ/156/241/table4>
- [7] Gaia DR3 Part 4. Variability (Gaia Collaboration, 2022)  
<https://vizier.cds.unistra.fr/viz-bin/VizieR?-source=I/358/>
- [8] The Czech Variable Star Catalogue, 2018, online data  
[Star catalog - VarAstro](#)
- [9] SIMBAD Astronomical Database - CDS (Strasbourg)  
<https://simbad.cds.unistra.fr/simbad/sim-id?Ident=%4017563784&Name=ATO%20J304.0966%2b52.4860&submit=submit>